Predicted High-Temperature Superconducting State in the Hydrogen-Dense Transition-Metal Hydride YH_3 at 40 K and 17.7 GPa

Duck Young Kim,[1,2] Ralph H. Scheicher,[2] and Rajeev Ahuja[2,3,*]

[1]*Theory of Condensed Matter Group, Cavendish Laboratory, University of Cambridge, Cambridge CB3 0HE, United Kingdom*
[2]*Condensed Matter Theory Group, Department of Physics and Materials Science, Uppsala University, Box 530, SE-751 21, Uppsala, Sweden*
[3]*Applied Material Physics, Department of Materials Science and Engineering, Royal Institute of Technology (KTH), SE-100 44, Stockholm, Sweden*

(Received 10 February 2009; published 10 August 2009)

Metallization in pure hydrogen has been proposed to give rise to high-temperature superconductivity at pressures which still lie beyond the reach of contemporary experimental techniques. Hydrogen-dense materials offer an opportunity to study related phenomena at experimentally achievable pressures. Here we report the prediction of high-temperature superconductivity in yttrium hydride (YH_3), with a T_c of 40 K at 17.7 GPa, the lowest reported pressure for hydrogen-dense materials to date. Specifically, we find that the face-centered cubic structure of YH_3 exhibits superconductivity of different origins in two pressure regions. The evolution of T_c with pressure follows the corresponding change of *s*-*d* hybridization between H and Y, due to an enhancement of the electron-phonon coupling by a matching of the energy level from Y-H vibrations with the peak of the *s* electrons from the octahedrally coordinated hydrogen atoms.

DOI: 10.1103/PhysRevLett.103.077002 PACS numbers: 74.10.+v, 63.20.kd, 74.25.Jb, 74.62.Fj

Hydrogen was predicted to become a metal and even a high-temperature superconductor when sufficiently pressurized, but, for the currently achievable pressure range, it continues to remain insulating. Certain hydrides might well be superconducting up to high critical temperatures and can become metallic at a lower pressure than hydrogen, presumably because of additive effects from chemical precompression [1]. Several theoretical and experimental efforts are currently underway to better understand the crystal structures and metallization process of such hydrides. Metallization in silane (SiH_4) was, for example, recently reported [2,3] and analyzed from a theoretical perspective by us [4]. Other high-T_c superconducting phases of hydrogen-dense materials have been computationally investigated: GeH_4 was predicted to have a T_c of 64 K at 220 GPa [5], SnH_4 could possess a T_c of 80 K at 120 GPa [6], and superconducting behavior was predicted in both layered SiH_4 [7] and AlH_3 [8].

Yttrium can form a hydride able to absorb about 300 mol % hydrogen, known to form hcp-structured YH_x at ambient pressure. This system undergoes an insulator-metal transition upon hydrogen uptake which has led to suggestions for possible applications as a switchable mirror [9]. The development of the diamond anvil cell technique facilitated investigations of the pressure dependence of YH_3 [10–13]. Raman [11] and infrared [12] studies found that fcc-structured YH_3 can exist at 10 GPa and is clearly stabilized around 25 GPa. It has been argued that another intermediate phase [13] or a coexisting hcp-fcc phase [14] could appear in the pressure range 10–25 GPa.

In this Letter, we focus on fcc-YH_3 [10–12,15], which is predicted to undergo a superconductor-metal-superconductor transition under pressure. Different degrees of *s*-*d* hybridization between hydrogen and yttrium as a function of pressure can resolve the underlying mechanism of the phase transition. Based on our calculations, fcc-YH_3 possesses lower enthalpy than the corresponding hcp structure for $P > 20$ GPa [16] and is dynamically stable starting from 17.7 GPa.

The computational studies presented here are based on the generalized gradient approximation [17] with the Perdew-Burke-Ernzerhof parametrization [18] for the exchange-correlation functional to density functional theory [19,20]. We employed the projector augmented wave (PAW) method [21], as implemented in the Vienna *ab initio* simulation package (VASP) [22] to calculate projected density of states. The PAW potential with the valence states $4s^2 4p^6 4d^1 5s^2 5p^0$ for Y has been employed with plane waves up to a cutoff energy of 1000 eV, and the density of states has been calculated with a $16 \times 16 \times 16$ *k*-point mesh generated by the Monkhorst-Pack (MP) method [23]. Phonon dispersion and electron-phonon calculations were performed with density functional perturbation theory [24] using the program QUANTUM ESPRESSO with a kinetic energy cutoff of 60 Ry and a $24 \times 24 \times 24$ MP mesh for Brillouin zone integration. Electron-phonon coupling matrix elements were computed in the first Brillouin zone on a $8 \times 8 \times 8$ *q* mesh. We calculated T_c using the Allen-Dynes equation [25]. To calculate phonon dispersion relations with the Fermi-Dirac broadening scheme, we employed the ABINIT code [26] with plane waves up to a cutoff energy of 50 Hartree and a $16 \times 16 \times 16$ MP *k*-point mesh.

Figure 1(a) displays a schematic of the fcc-YH_3 crystal structure at 17.7 GPa combined with an electron localiza-

tion function plot. As can be seen, there exist one type of yttrium atom occupying the fcc site and two types of hydrogen: H(1) and H(2), tetrahedrally and octahedrally coordinated, respectively. As the nearest neighbor of Y, H(1) forms a bond with Y [Fig. 1(a)]. In contrast, H(2) participates only weakly in the bonding network and is essentially isolated. The strongly localized electron of H(2) results in a virtually dispersionless narrow band. Y and H(1) thus form a "cage," effectively trapping H(2) inside. The stability of the cage structure upon removal of H(2) was tested by us through structural relaxation, and no significant change in the geometry was found. As a consequence, H(2) can essentially be removed from the YH_3 crystal without strongly affecting the cage structure.

In Figs. 1(b)–1(e), we compare the electronic density of states (DOS) for each element at three pressure values (15, 30, and 45 GPa); the peak shift of Y starts from 0.10 eV above E_F to 0.15 eV, while the peak shift of H density ranges from 0.02 to 0.10 eV. Since phonon energies of interest are typically within 0.10 eV, the change in the H(2)-associated DOS is of critical importance for electron-phonon coupling, as we discuss in greater detail below.

The dynamical stability as obtained from the phonon dispersion relation was analyzed as a function of pressure (Fig. 2). For $P < 17.7$ GPa, imaginary frequencies emerge, rendering fcc-YH_3 dynamically unstable. The Fermi surface is formed around Γ (a closed shape) and L. Figure 2(a) displays a stabilized phonon dispersion relation at 17.7 GPa and the lowest acoustic mode at 15 GPa, which is destabilized near K. The mechanism driving the softening of the K-mode phonon (e.g., 3/4, 3/4, 0) is closely related with the electronic momentum transfer between near L points (1/2, 1/2, 1/2) and (−1/2, −1/2, 1/2).

Our zero-temperature calculations demonstrate that fcc-YH_3 is unstable below 17.7 GPa, preceded by the onset of phonon softening. Once finite-temperature effects are included, we find that dynamical instabilities in the phonon dispersion disappear [Fig. 2(b)]. This result opens the possibility that finite temperature may allow fcc-YH_3 to be dynamically stabilized even for pressures below 17.7 GPa.

Based on our first-principles calculations assessing the electron-phonon coupling strength λ, we predict high-temperature superconductivity in fcc-YH_3. As can be seen in Fig. 3(a), the trend of T_c in YH_3 with increasing pressure is different from that in pure Y [27], while the change of the d state in pure Y (governing the superconducting nature) is the same as in fcc-YH_3 [28], indicating different origins of superconductivity in Y and YH_3.

As shown above, H(2) possesses a sharp peak in the corresponding projected DOS at the Fermi level for a pressure around 17.7 GPa, closely intertwining it with the superconducting behavior. This peak shifts towards higher energy as the pressure is raised, due to hybridization with other atoms causing the atomlike narrow band to increase in width. The T_c at the lowest possible pressure at which fcc-YH_3 is still dynamically stabilized is remarkably high, namely, around 40 K, based on our calculations [Fig. 3(a)].

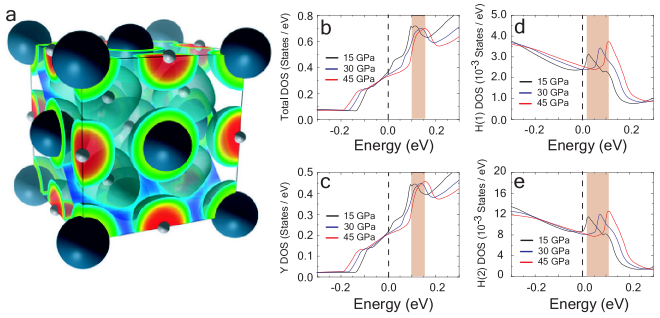

FIG. 1 (color online). (a) Crystal structure and electron localization function plot at 17.7 GPa. Blue spheres represent yttrium, while white small spheres represent hydrogen, with H(1) at tetragonal sites and H(2) at octahedral sites. (b) Total DOS and projected DOS per atom onto (c) Y, (d) H(1), and (e) H(2) near E_F for three different pressure values. The vertical dashed line indicates the position of the Fermi level. Shaded regions show the peak shift with pressure.

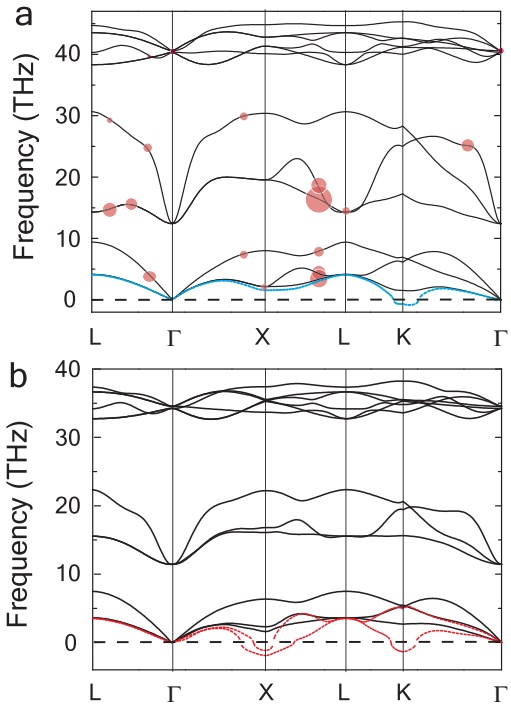

FIG. 2 (color online). (a) Representative phonon dispersion curves at 17.7 GPa shown as solid lines with the blue dashed line corresponding to the lowest acoustic mode at 15 GPa. Red circles mark electron-phonon coupling with the radius proportional to their respective strength. (b) Phonon dispersion curves at 13 GPa with zero electronic temperature shown as red dashed lines [only the two lowest acoustic branches are shown, which are destabilized near X and K; the softening near X (1, 0, 0) is closely related with the momentum transfer between the nearest L points], and a full set of dispersion curves where 0.01 Hartree electronic temperature has been added (solid lines). The corresponding physical temperature can be orders of magnitude smaller, as recently shown by us on the example of another hydrogen-rich material [30].

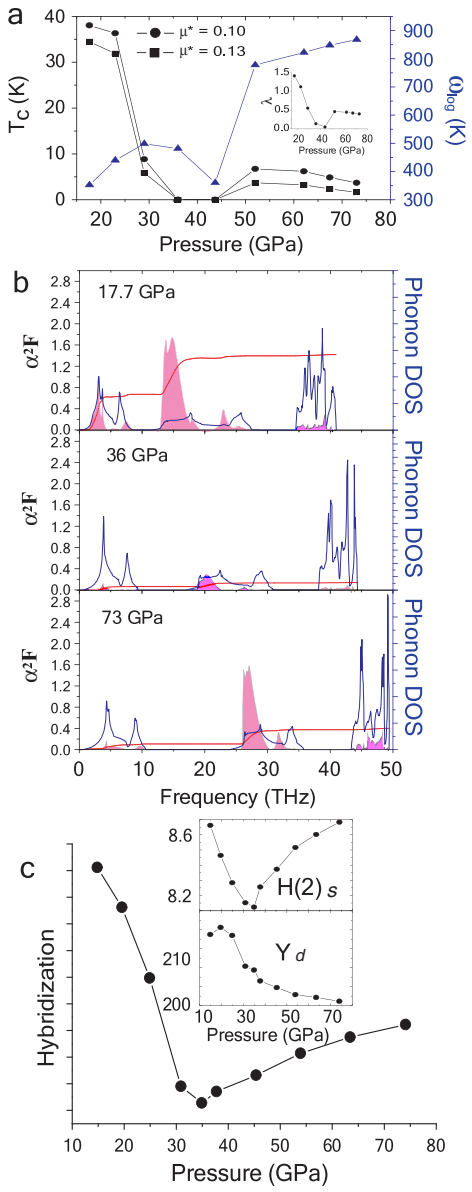

FIG. 3 (color online). (a) Pressure dependency of T_c and $\omega_{\log}$. The inset shows the evolution of the electron-phonon coupling constant λ with pressure. (b) The spectral function α^2F (red shaded area), integrated λ (red line), and phonon DOS (blue curves) as a function of frequency at $P = 17.7$, 36, and 73 GPa, respectively. (c) Hybridization between the d state of Y and the s state of H(2) at the Fermi level as a function of pressure. Plotted in the inset is the DOS (in units of states/atom/meV) at the Fermi level for H(2) s electrons (upper panel) and for Y d electrons (lower panel).

In our estimation for T_c, we have tested two different values of the Coulomb pseudopotential μ^*: 0.10 and 0.13, the latter having been proposed by Ashcroft for hydrogen-dense materials [1]. We find a steep drop in T_c at a pressure of around 25 GPa [Fig. 3(a)], which is a precursor for a transition from a superconducting to a normal metallic state, and fcc-YH_3 remains in the metallic state until 45 GPa, where the superconducting behavior reemerges as the pressure is raised higher.

This superconducting-metallic-superconducting behavior (here we use the term "metallic" in the sense that the system is *only* metallic and not superconducting) can be understood as follows. At lower pressure, the high T_c is made possible by the atomiclike s band from H(2) at the Fermi level [upper panel of Fig. 3(b)]. In this pressure regime, the peak of the DOS at 15 GPa near the Fermi level of H(2) locates within ≈5 THz [Fig. 1(e)], which corresponds to the range of Y vibrational frequencies [Fig. 3(b)]. Half of the electron-phonon coupling λ results from this frequency range, while the remainder is due to the higher frequency regime Y-H(2). It is worth noting that the electron-phonon coupling appears near L and Γ in Fig. 2(a), in close proximity to the Fermi surface, with coupling near L contributing particularly strong to λ. In the intermittent metallic region (25–45 GPa), the spectral function is essentially zero [middle panel of Fig. 3(b)], and the superconducting state ceases to exist. The peak in the lower panel of Fig. 3(b) shifts to frequencies above the Y-vibration mode regime (≈10 THz), and strong electron-phonon coupling can no longer be expected [also, the Y-H(2) vibration regime is located around 20 THz]. However, above 50 GPa, H(2) can form bonds with the d state of Y, thus gaining again the chance to become superconducting. The DOS peak in Fig. 1(e) matches with the second regime in the lower panel of Fig. 3(b) in that Y is no longer contributing to electron-phonon coupling, but Y-H(2) hybridization becomes important. T_c is expected to be lower than in the first region, because the phonon frequencies shift towards higher energies, reducing the amplitude of the normalized weighting function in Eliashberg theory [29]. Also shown in Fig. 3(b) is the phonon DOS containing three major regions: The lower-frequency region is dominated by Y, the medium-frequency region corresponds to Y-H(2) interactions, and the high-frequency region is a result of H(1) vibrations. Here again, H(2) plays a key role, in the sense that increasing pressure induces hybridization of its s state with the d state of Y, forming stronger bonds.

Such a behavior becomes even more apparent when viewing the V-shaped curve in Fig. 3(c). In the first region (below 25 GPa), where the s state of H(2) at the Fermi level is decreasing, H(2) exists as an atomiclike hydrogen in the system and, as described above, interacts rather weakly with the surrounding host structure. The octahedrally coordinated H(2) atoms can thus be removed easily without affecting the crystal structure. Once the minimum in the s-state density at the Fermi level is reached, the s state has been transformed from a narrow atomic band to a much broader band, thus giving rise to the metallic state which has been observed in this pressure region (around 25 GPa), in excellent agreement with experimental findings showing that the metallic fcc phase appears above 25 GPa [11,12]. Eventually, as the pressure is increased further, the s state at the Fermi level starts to rise again, due to the hybridization of the H(2) s state with the d state of Y. The product of the respective densities at E_F of the H(2) s state and the Y d

state [Fig. 3(c)] mirrors in fact the pressure dependence of T_c in fcc-YH_3.

As mentioned above, pure Y exhibits a monotonic behavior of T_c under pressure [27]. The V-shaped curve shown by us thus indicates that the origin of superconductivity in YH_3 cannot be explained by a change in the conducting d electrons. According to the McMillan formula, T_c is governed by three parameters: coupling-weighted phonon momentum ($\omega_{\log}$), electron-phonon coupling (λ), and conduction electrons near E_F. Conduction electrons near E_F are ruled out as the main contributor for the superconductivity behavior, since there exists only a low density of Y d electrons and even lower H s electrons. The change in $\omega_{\log}$ under pressure is seen to be inconsistent with that of T_c. This leaves electron-phonon coupling (λ) as the dominant factor for affecting T_c. We thus explain the similarity between the respective behaviors of T_c and the hybridization function under pressure to be due to the enhancement of electron-phonon coupling by the match of the energy level from Y-H(2) vibrations with the peak of H(2) s electrons. The peak of Y d electrons is located too high above E_F, and the density of H(2) s electrons is richer than that of H(1) [due to the existence of strong bonds between Y-H(1) throughout the entire studied pressure range], both of which are located close to the E_F and can therefore contribute strongly to the electron-phonon coupling.

In summary, we have shown that fcc-YH_3 is the ground state structure above 20 GPa and dynamically stable above 17.7 GPa, with finite-temperature effects stabilizing it at even lower pressure. Experimentally, it has been suggested that semiconducting fcc-YH_3 can be formed at 10 GPa and transferred into a metallic phase without structural transformation. This phase of YH_3 is predicted by us to be superconducting with a high T_c of 40 K at 17.7 GPa and to become normal metallic (i.e., nonsuperconducting) near 25 GPa. This hitherto unprecedented low pressure puts superconducting YH_3 into much closer experimental reach than comparable hydrogen-rich superconductors. It should be noted, however, that due to the metastability near the threshold pressure (17.7 GPa), it might be necessary in experiments to approach this state via a rapid decompression (quenching) technique. Metallic YH_3 reenters the superconducting regime at 45 GPa (albeit with lower T_c).

This work was supported by the Swedish Foundation for International Cooperation in Research and Higher Education (STINT), the Swedish Research Council (VR), Futura Foundation, Göran Gustafsson Stiftelse, and Wenner-Gren Stiftelserna. Swedish National Infrastructure for Computing (SNIC) and Uppsala Multidisciplinary Center for Advanced Computational Science (UPPMAX) provided computing time.

*rajeev.ahuja@fysik.uu.se

[1] N. W. Ashcroft, Phys. Rev. Lett. **92**, 187002 (2004).
[2] X.-J. Chen, V. V. Struzhkin, Y. Song, A. F. Goncharov, M. Ahart, Z. Liu, H.-k. Mao, and R. J. Hemley, Proc. Natl. Acad. Sci. U.S.A. **105**, 20 (2008).
[3] M. I. Eremets, I. A. Trojan, S. A. Medvedev, J. S. Tse, and Y. Yao, Science **319**, 1506 (2008).
[4] D. Y. Kim, R. H. Scheicher, S. Lebégue, J. Prasongkit, B. Arnaud, M. Alouani, and R. Ahuja, Proc. Natl. Acad. Sci. U.S.A. **105**, 16 454 (2008).
[5] G. Gao, A. R. Oganov, A. Bergara, M. Martinez-Canales, T. Cui, T. Iitaka, Y. Ma, and G. Zou, Phys. Rev. Lett. **101**, 107002 (2008).
[6] J. S. Tse, Y. Yao, and K. Tanaka, Phys. Rev. Lett. **98**, 117004 (2007).
[7] X.-J. Chen, J.-L. Wang, V. V. Struzhkin, H. kwang Mao, R. J. Hemley, and H.-Q. Lin, Phys. Rev. Lett. **101**, 077002 (2008).
[8] I. Goncharenko, M. I. Eremets, M. Hanfland, J. S. Tse, M. Amboage, Y. Yao, and I. A. Trojan, Phys. Rev. Lett. **100**, 045504 (2008).
[9] J. N. Huiberts, R. Griessen, J. H. Rector, R. J. Wijngaarden, J. P. Dekker, D. G. de Groot, and N. J. Koeman, Nature (London) **380**, 231 (1996).
[10] R. Ahuja, B. Johansson, J. M. Wills, and O. Eriksson, Appl. Phys. Lett. **71**, 3498 (1997).
[11] T. Kume, H. Ohura, S. Sasaki, H. Shimizu, A. Ohmura, A. Machida, T. Watanuki, K. Aoki, and K. Takemura, Phys. Rev. B **76**, 024107 (2007).
[12] A. Ohmura, A. Machida, T. Watanuki, K. Aoki, S. Nakano, and K. Takemura, Phys. Rev. B **73**, 104105 (2006).
[13] A. Machida, A. Ohmura, T. Watanuki, K. Aoki, and K. Takemura, Phys. Rev. B **76**, 052101 (2007).
[14] T. Palasyuk and M. Tkacz, Solid State Commun. **133**, 477 (2005).
[15] S. J. van der Molen, D. G. Nagengast, A. T. M. v. Gogh, J. Kalkman, E. S. Kooij, J. H. Rector, and R. Griessen, Phys. Rev. B **63**, 235116 (2001).
[16] J. S. de Almeida, D. Y. Kim, C. Ortiz, M. Klintenberg, and R. Ahuja, Appl. Phys. Lett. **94**, 251913 (2009).
[17] J. P. Perdew, J. A. Chevary, S. H. Vosko, K. A. Jackson, M. R. Pederson, D. J. Singh, and C. Fiolhais, Phys. Rev. B **46**, 6671 (1992).
[18] J. P. Perdew, K. Burke, and M. Ernzerhof, Phys. Rev. Lett. **77**, 3865 (1996).
[19] P. Hohenberg and W. Kohn, Phys. Rev. **136**, B864 (1964).
[20] W. Kohn and L. J. Sham, Phys. Rev. **140**, A1133 (1965).
[21] P. E. Blöchl, Phys. Rev. B **50**, 17 953 (1994).
[22] G. Kresse and J. Furthmüller, Phys. Rev. B **54**, 11 169 (1996).
[23] H. J. Monkhorst and J. D. Pack, Phys. Rev. B **13**, 5188 (1976).
[24] S. Baroni, S. de Gironcoli, A. Dal Corso, and P. Giannozzi, Rev. Mod. Phys. **73**, 515 (2001).
[25] P. B. Allen and R. C. Dynes, Phys. Rev. B **12**, 905 (1975).
[26] X. Gonze *et al.*, Comput. Mater. Sci. **25**, 478 (2002).
[27] J. J. Hamlin, V. G. Tissen, and J. S. Schilling, Phys. Rev. B **73**, 094522 (2006).
[28] Z. P. Yin, S. Y. Savrasov, and W. E. Pickett, Phys. Rev. B **74**, 094519 (2006).
[29] P. B. Allen, Phys. Rev. B **6**, 2577 (1972).
[30] D. Y. Kim, R. H. Scheicher, and R. Ahuja, Phys. Rev. B **78**, 100102 (2008).